

RESEARCH

Open Access



Characterization of Electrical Heating of Graphene/PLA Honeycomb Structure Composite Manufactured by CFDM 3D Printer

Hyelim Kim¹ and Sunhee Lee^{2*} 

*Correspondence:

shlee014@dau.ac.kr

² Professor, Department of Fashion Design, Dong-A University, Busan 49315, South Korea

Full list of author information is available at the end of the article

Abstract

Conveyor fused deposition modelling (CFDM) 3D printing of graphene (GR)/polylactic acid (PLA) composite filament offers a unique capability to manufacture tailorable honeycomb structures which can be designed and optimized for specific applications. Among the various filaments that can be used for 3D printing, PLA, carbon black (CB)/PLA, and GR/PLA filaments were collected and then examined by differential scanning calorimetry (DSC), thermal gravity analysis (TGA), and Raman spectra. A stereolithography (STL) file with a 3D honeycomb structure model was prepared and transformed into a G-code file using a G-code generator. The extrusion conditions for CFDM 3D printing were controlled by infill and print speed. PLA, CB/PLA, and GR/PLA composite honeycomb samples were manufactured by 3D printing based on FDM using PLA, CB/PLA, and GR/PLA filaments. CFDM 3D printed honeycomb samples prepared by PLA, CB/PLA and GR/PLA filament were analyzed for morphology, surface resistance, electrical heating properties. For the 3D printed honeycomb structure sample using CB/PLA and GR/PLA, the optimum condition was set up 230 °C and 220 °C respectively of the printer temperature, 50 °C of bed temperature, and 30 mm/s of printer speed. Surface resistivity of honeycomb structure sample using CB/PLA and GR/PLA is about 299.0 Ω/sq and 118.0 Ω/sq. The maximum surface temperature of honeycomb structure sample using CB/PLA and GR/PLA is ca. 78.7 °C and 143.0 °C applied to 25 V.

Keywords: CFDM 3D printer, Graphene/PLA, Honeycomb, Fine structure, Electrical properties

Introduction

Conveyor fused deposition modeling (CFDM) 3D printing process is a one of new technology of FDM 3D printing, which can be provided new possibilities, like long printings and producing series production. Several studies are studied to apply 3D printing technology to textiles (Grimmelsmann et al. 2018; Kim and Kim 2018; Kim et al. 2019a; Lee 2019; Mpofu et al. 2019), existing FDM 3D printing technology is difficult to manufacture in large quantities due to limit of bed size and nozzle movement. CFDM 3D printing technology has complimented these parts and can be applied to mass production of fabrics by improving productivity through continuous process. BLACKBELT 3D printer

(Black belt 3D printer, 2019) is a representative CFDM 3D printer. It is designed to enable continuous process by combining unique conveyor belt type bed technology with FDM 3D printer. That bed is moved horizontally to provide every new Z-axis and print substrate. Thus, samples can be printed continuously.

Nowadays, to fabricate 3D printed flexible electronics with FDM 3D printer, conductive filaments are developed by mixing with thermoplastic polymers such as polylactic acid (PLA), thermal polyurethane (TPU) or acrylonitrile butadiene styrene (ABS) and carbon nano-based materials such as carbon black (CB), carbon nanofiber (CNF), carbon nanotube (CNT) or graphene (GR) (Guo et al. 2019; Kamyshny and Magdassi 2019). To 3D print wearable electronics, it is reported that carbon-based polymer composites are advantageous over metal-based 3D printed wearable electronics due to possible to print with FDM printer and easy to product manufacturing (Kwok et al. 2015). Using carbon nano-based 3D filaments, research on 3D printed electrode components, circuits, sensors, and the like continues (Flowers et al. 2017; Kim et al. 2019c; Kwok et al. 2015). Graphene is one of carbon nano-based materials, it has a single-atom-thick sp^2 carbon crystal. Its two-dimensional honeycomb structure exhibiting many unique properties, such as high mechanical strength, large specific surface area, high thermal conductivity and excellent electrical conductivity (Wei et al. 2015; Yu et al. 2017). Graphene-based filaments having those unique characteristics have been studied in the field of 3D printing electronics (Foster et al. 2017; Ivanov et al. 2019; Zhang et al. 2016; Zhuang et al. 2017).

Zhang et al. (2016) was reported fabrication of flexible circuits using GR/PLA filament by FDM 3D printing. The conductivity of samples was gradually increased with adding graphene contents, when the 8% graphene was used in GR/PLA filament and 3D printed GR/PLA circuit, those were reached to 0.36 S/cm and 4.76 S/cm, respectively. Zhuang et al. (2017) was studied the distribution of the amorphous materials' components of objects with anisotropic heat distribution using PLA and GR/PLA filaments by FDM 3D printing. Used 3D printer could extrude and melt two kinds of filaments into one nozzle, and the extrusion ratio of the two types of filaments was adjusted. As the extrusion ratio of PLA and GR/PLA filament increased, the thermal stability and conductivity were improved. In addition, as the PLA and GR/PLA extrusion ratio increased from 1:19 to 19:1, the surface temperature increased linearly, the maximum temperature was reported to be about 30 °C at 10 V and 90 °C at 25 V, respectively. As showed in the previous studies, studies on 3D printed wearable electronics such as circuits, sensors, and heat distribution using graphene filaments are being conducted. However, it is confirmed that studies on mass production and continuous processes that can be applied to smart clothing have been insufficient.

Our research team have studied fabric heating elements by various coating method coated on cotton fabrics, polyester fabrics, flame retardant cotton fabrics, and aramid knits using conductive inks such as CNF/polymer composites and GR/polymer composites (Kim and Lee 2018a, b, 2019a, b; Kim et al. 2019b). Based on previous studies, this study is a basic research for manufacturing a fabric heating element applying a 3D printed sample having an electric heating performance, a 3D printing sample having a honeycomb structure was manufactured using a RAW PLA filament and two types conductive filament by CFDM 3D printer. The specific purposes are as follows. First, DSC, TGA, and Raman spectra were measured to characterize conductive carbon black (CB)/

PLA filament and graphene (GR)/PLA filament. Secondly, 3D modeling of a honeycomb structure having a size of 50 mm × 50 mm × 2 mm was performed by 3D modeling program, and then converted to G-code for printing, and samples were printed based on the characteristics of each filament. Finally, to confirm the properties of the three printed samples, morphology, surface resistance and electrical heating properties were studied.

Methods

Materials

Table 1 shows the specifications of selected materials, PLA (eSun Ltd, China), carbon black (CB)/PLA (Proto-pasta Ltd, USA), and graphene (GR)/PLA (Blackmagic, Ltd, USA) filament in this study. Among FDM technology-based 3D printing materials, and their diameter was 1.75 mm. The filaments were stored inside the desiccator at a standard temperature before being used for analysis and 3D printing.

Preparations of 3D printed honeycomb structure

To fabricate honeycomb structures, a modeling with a size of 50 mm × 50 mm × 2 mm was created by repeating hexagonal patterns using the 123D design program. The obtained modeling file was converted to a STL file, which was transformed into the G-code file format to be ready for CFDM 3D printing. Scheme of honeycomb structure and 3D modeling is shown in Fig. 1.

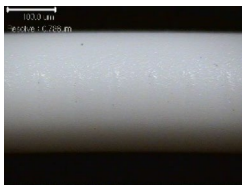
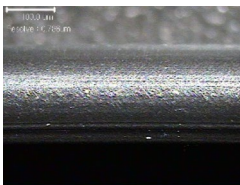
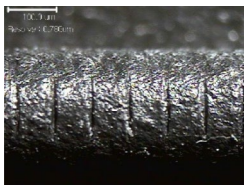
CFDM 3D printing conditions

In this study, CFDM 3D printer (Blackbelt Ltd, Netherland) was used for honeycomb structure with various filaments. In Table 2, we summarized the 3D printing conditions after pre-test with various filaments. Three samples were printed by controlling the printing temperature, layer height, and printing speed.

Characterizations

To analyze 3D filaments for 3D printing process, the thermal analysis was done with differential scanning calorimetry (DSC, DSC Q 25, TA instruments, USA) and thermogravimetric analysis (TGA, TGA Q500 V20.10 Build 36, TA instruments, USA). DSC was performed with the heating rate of 10 °C/min and the temperature measurement range of 30–200 °C, 1st curves of 3D filaments were obtained. From these

Table 1 Specification of materials using in this study

	PLA	CB/PLA	GR/PLA
Diameter (mm)	1.75	1.75	1.75
Density (g/cm ³)	1.21	1.15	–
Conductivity (Ω/cm)	–	15	0.6
Surface image			

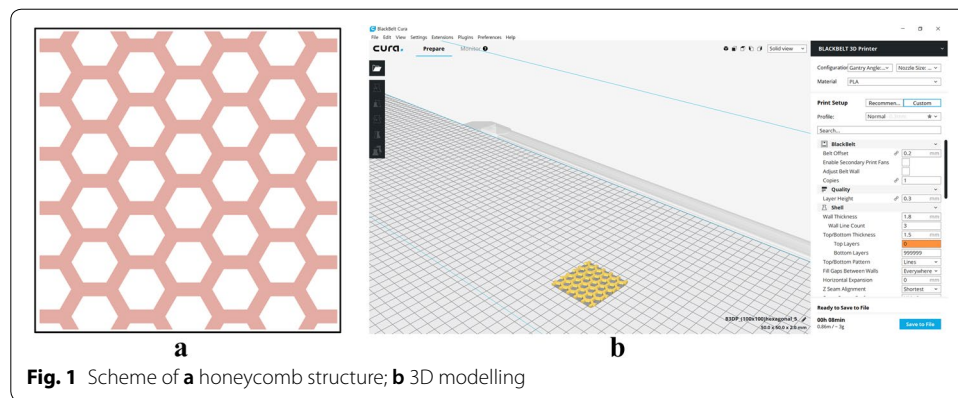


Fig. 1 Scheme of **a** honeycomb structure; **b** 3D modelling

Table 2 CFDM 3D printing conditions with various filaments

	PLA	CB/PLA	GR/PLA
Belt offset (mm)	0.2	0.2	0.2
Layer height (mm)	1.8	1.8	1.8
Temperature of nozzle (°C)	215	230	220
Temperature of bed (°C)	75	50	50
Printing speed (mm/s)	40	30	30
Infill speed (mm/s)	30	22.5	22.5
Infill (%)	100	100	100

curves, the glass temperatures, melting temperatures and crystallization temperatures were confirmed. The weight of sample was 3 mg. TGA was conducted under nitrogen atmosphere at a heating range of 30–800 °C with heating rate 20 °C/min. The sample weight was 10 mg. Raman spectra (XperRam 200, Nano Base, Korea) was acquired with laser wavelength of 532 nm, laser power of until 3.0 mW. Scan range was from 3000 cm^{-1} to 500 cm^{-1} and scan time was 16–512 s/each.

To investigate of honeycomb structure, the surface characteristics analysis was done with the digital camera and fabric microscope (NT 100, Nextec, Korea) with $\times 6.5$ magnification. Surface resistance was measured with multimeter (ST850A, Saehan Tester, Co. Ltd., Korea) based on the AATCC-76 method. Two parallel conductive probe were placed in contact with both edges of the samples. The surface resistance (R_s) was calculated as Eq. (1):

$$R_s (\Omega/\text{sq}) = (W/D) \times R \quad (1)$$

where R is resistance measured by the multimeter, W is the width of the sample, and D is the distance between the two electrodes. Electrical heating performance of the samples with honeycomb structure was determined based on surface temperature with various applied voltages while using a DC power supply (CPS-2450B, CHUNGPA EMT Co. Ltd., Korea). Both edges of samples were connected to the alligator clips. The range of applied voltage was from 5 to 50 V with 5 V (DC) intervals for 3 min. A thermal imaging camera

(FLIR i5, FLIR Systems INC., USA) was used to measure the surface temperature after applying different voltages.

Results and discussion

DSC curves of PLA, carbon black/PLA, and graphene/PLA filaments for 3D printing

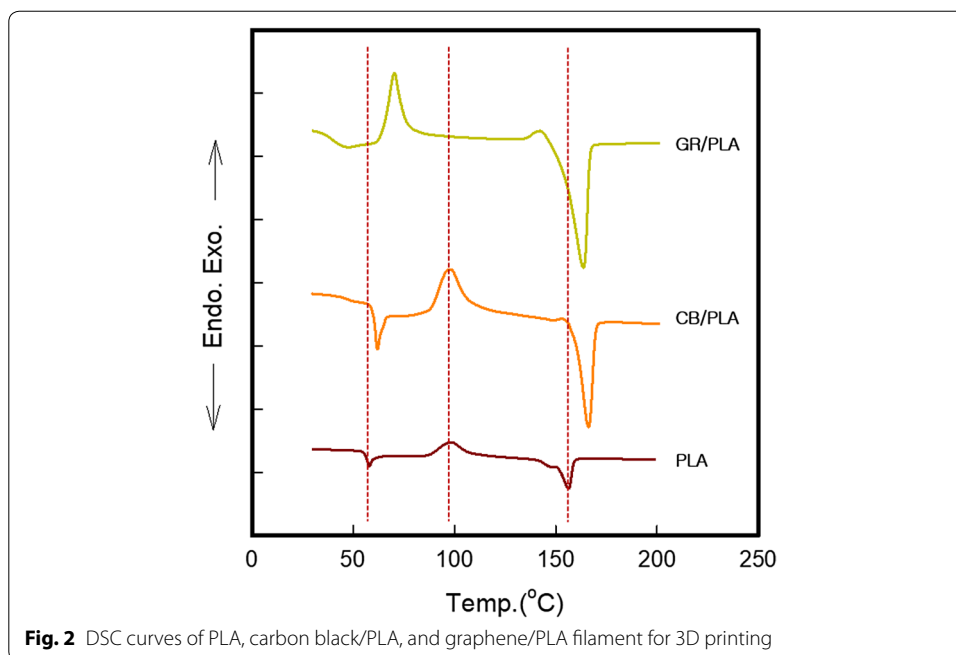
To analyze thermal properties of three types of FDM 3D filaments, PLA, CB/PLA, and GR/PLA filaments for 3D printing, the DSC curves shown in Fig. 1. Three types of FDM filaments demonstrate several typical thermal peaks during heating, such as glass transition, T_g , melting temperature, T_m , and cold crystallization, T_{cc} . These peaks of PLA, CB/PLA, and GR/PLA filaments are presented in Table 3. In case of PLA filament during heating, T_g , T_{cc} , and T_m small peak were indicated at 59.3 °C, 99.6 °C, and 156.7 °C, respectively. The small crystallization and the melting peak for the PLA filament indicate that the homopolymer is difficult to be crystallized from glassy state (Kotsilkova et al. 2019). In DSC curve of CB/PLA filament, T_g , T_{cc} , and T_m peaks were found at 61.9 °C, 98.2 °C, and 166.2 °C, respectively. In case of three thermal peaks of CB/PLA filament, the peak intensities were larger than PLA filament and T_g and T_m peaks were shifted up to higher temperature and T_{cc} peak was shifted down to lower temperature. In case of GR/PLA filament, T_g , T_{cc} , and T_m peaks were found at 44.2 °C, 70.3 °C, and 163.8 °C, respectively. While the size of the T_g peak was decreased, the size of the peaks of T_{cc} and T_m was found to be higher than that of the PLA and CB/PLA filaments. In addition, it was confirmed that T_g and T_{cc} shifted to lower temperature and T_m moved to higher temperature in the PLA filament to which GR was incorporated. By addition of CB and GR to PLA, a cold crystallization and the crystalline phase transition from crystal form are induced (Kotsilkova et al. 2019). It indicates that both carbon nanofillers could be formed the crystallization of the PLA from glassy state. The value of ΔH of CB/PLA and GR/PLA indicated 22.6 J/g and 33.4 J/g, respectively. It shows remarkably increased than PLA filaments. In addition, T_m of the CB/PLA and GR/PLA filaments is shifted up to higher temperatures compared to the PLA. Also, T_m of the CB/PLA filament is higher than that of GR/PLA filament, the which is associated with melting of large portion of crystals in composites, which are formed due to the nucleation effect of carbon nanofillers. Therefore, it was confirmed that T_m increased because CB/PLA and GR/PLA filaments showed more crystalline region than PLA, and CB/PLA filament developed more crystalline region than GR/PLA due to the nucleation effect.

TGA curves of carbon black/PLA and graphene/PLA filaments for 3D printing

To compare thermal properties for CB/PLA and GR/PLA filaments, the TGA curves presented in Fig. 2. In Fig. 2a, three stages of weight loss of CB/PLA were indicated.

Table 3 Thermal properties of PLA, carbon black/PLA, and graphene/PLA filament for 3D printing

	PLA	CB/PLA	GR/PLA
T_g (°C)	59.3	61.9	44.2
T_{cc} (°C)	99.6	98.2	70.3
T_m (°C)	156.7	166.2	163.8



As the temperature increased, the first significant weight loss was revealed between at 180 °C and 300 °C, which can be indicated the decomposition of PLA. Another significant weight loss was observed between about 400 °C and 500 °C. The residual weight of CB/PLA filaments was found at 500 °C to 800 °C with 20.19%. This is found to correspond to carbon black which has good thermal property. As shown in Fig. 2b, GR/PLA filament indicated two stages of weight loss in the TGA curve about 6.63% and 77.62% at around 180 °C to 300 °C and 300 °C to 400 °C, respectively. Those stages of weight loss indicated the small molecules and the decomposition of PLA. After 400 °C to 800 °C, a residual weight of 15.11% remained, indicating that the graphene, which has good thermal properties, did not decompose (Yu et al. 2017; Zhuang et al. 2017). Based on TGA data, the content of graphene in the GR/PLA filament was about 15%. The residue of the CB/PLA and GR/PLA filaments at 230 °C and 220 °C which the highest temperature during 3D printing processing was higher than around 99%, indicating that the composites hardly decomposed at or below those temperature. Thus, both filaments were not seriously decomposed and damaged during the 3D printing processing, which confirmed those temperatures were a suitable temperature for CFDM 3D printing (Fig. 3).

Raman spectra of carbon black/PLA and graphene/PLA filaments for 3D printing

Raman spectroscopy provides a powerful method for the characterization of carbon materials such as carbon black, carbon nanotube and graphene (Bokobza et al. 2008). It also can be used to determine the number of graphene layers and its structural quality either at a pure state or dispersed in the polymer matrix. This data can be obtained by analyzing the intensity, shape and bands peak position (Bokobza et al. 2015; Ivanov et al. 2019). In general, carbon black has two broad peaks around at 1350 cm^{-1} and at 1600 cm^{-1} , respectively. In Fig. 4, the Raman spectra of CB/PLA filament also indicated two main broad peaks located at about 1350 cm^{-1} and at 1600 cm^{-1} associated with

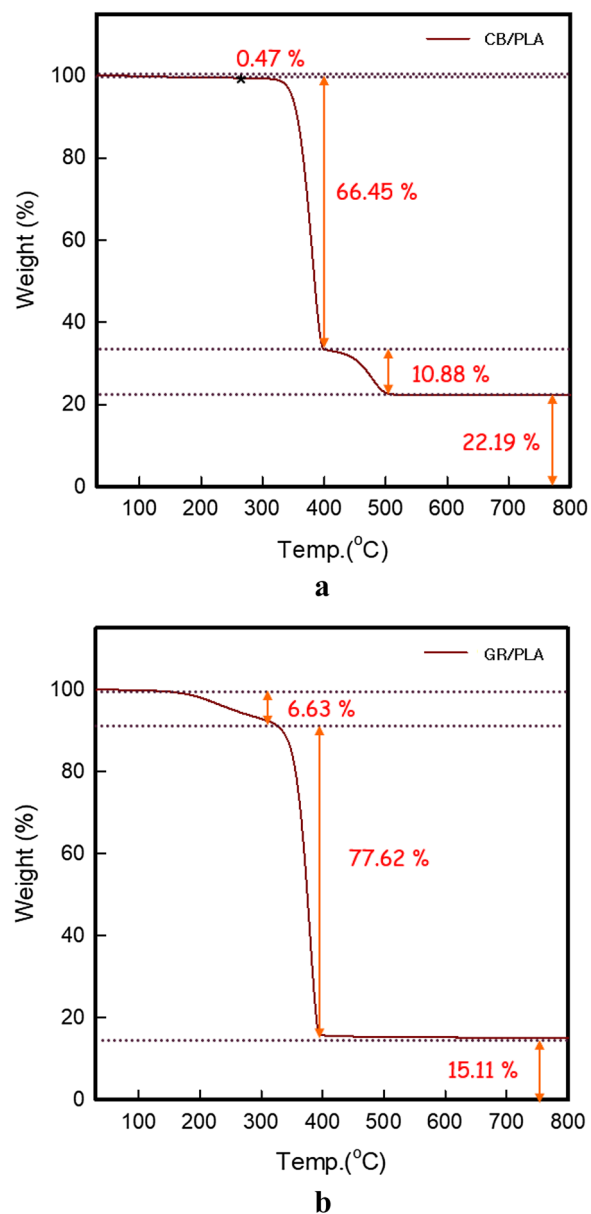
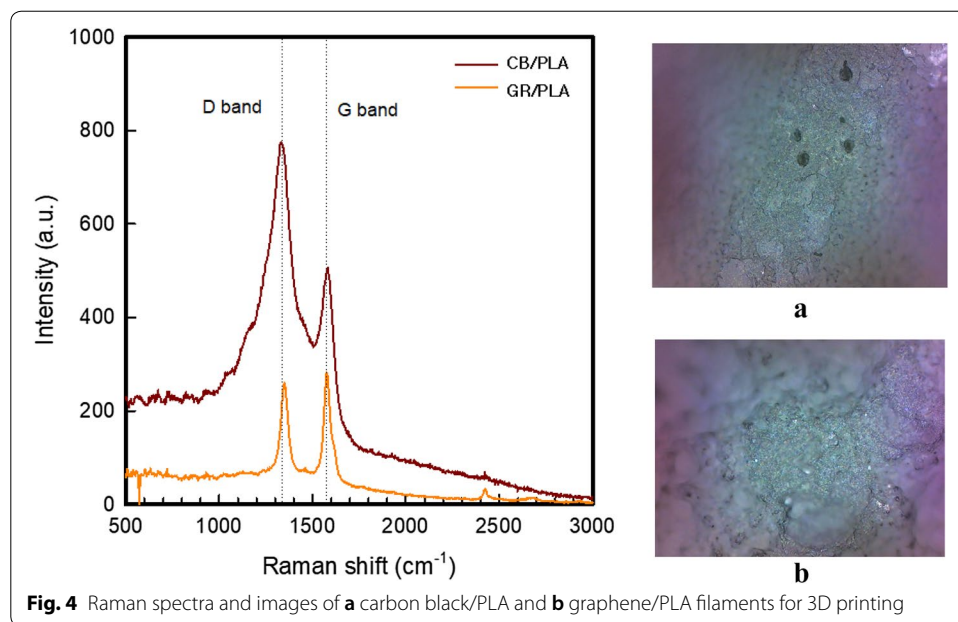


Fig. 3 TGA curves of **a** carbon black/PLA and **b** graphene/PLA filament for 3D printing

D band and G band, respectively. In case of graphene spectrums, those are characterized by three principle vibration bands designed as the G, D, and 2D band (Azi et al., 2019). The G band is the representative of an in-plane vibrational mode of sp^2 hybridized carbon atoms of graphene sheets. The intensity and position of G band is sensitive to the number of graphene layers so that this band appears in lower energy region with more intensity while layer thickness increases. The D band represents disorder or defects in the graphene carbon lattice, and is corresponding to sp^3 -bonded carbon. In Fig. 4, GR/PLA filament shows the three major Raman signals can be identified. D band at 1353 cm^{-1} which corresponds for defected graphite, and the G band at 1587 cm^{-1} which associated graphite, and 2D band around at 2696 cm^{-1} which corresponds to a



few layers of graphene. This data shows that the graphitic materials doped PLA is comprised of several graphitic layers. This data shows that the conductive PLA is comprised of carbon black and graphene composite, and GR/PLA made with several graphene layers. Additionally, intensity ratios such as I_D/I_G give an insight of structural disorder degree and quality of graphene, where defect-free ratio is equal 2 (Ivanov et al. 2019). The I_D/I_G ratio for GR/PLA revealed lower than CB/PLA indicated, thus, G/PLA indicated more surface integrity.

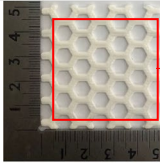
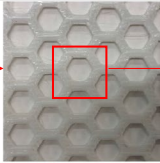
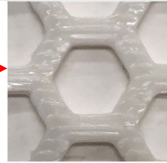

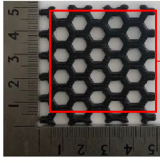
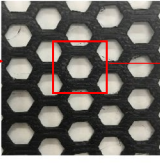
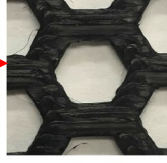

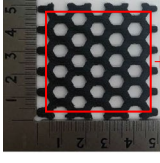
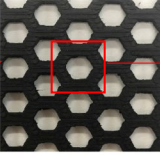


Morphology of 3D printed honeycomb samples

To investigate morphology of 3D printed honeycomb samples with FDM printer, Table 4 shows digital images and surface morphology of samples. We designed and printed three-dimensional honeycomb structures as the left digital images using PLA, CB/PLA, and GR/PLA, respectively. The dimensions of samples fixed 50 mm × 50 mm × 2 mm. At high magnification digital images and surface morphology, the results can be seen that PLA 3D printed honeycomb samples are more luster than CB/PLA and GR/PLA 3D printed honeycomb samples. Whereas, in the GR/PLA 3D printed honeycomb sample, the gloss was reduced than the other two samples, it is confirmed that the graphene was added to PLA to produce a brittle composite than PLA 3D printed honeycomb sample.

Surface resistance of 3D printed honeycomb samples

The surface resistance of 3D printed honeycomb samples with PLA, CB/PLA, and GR/PLA shown in Fig. 5 and Table 5. In general, it has been reported that carbon nanomaterials have different electrical properties depending on their orientation (Ladani et al. 2016). In the 3D printing process, the printing direction of the samples are determined by the direction in which the nozzle moves (Dorigato et al. 2017). In this study, the surface resistance of the machine direction (MD) and the cross direction (CD) was measured to determine

Table 4 Morphology of 3D printed honeycomb samples

Sample	Digital images			× 6.5 magnification
PLA				
CB/PLA				
GR/PLA				

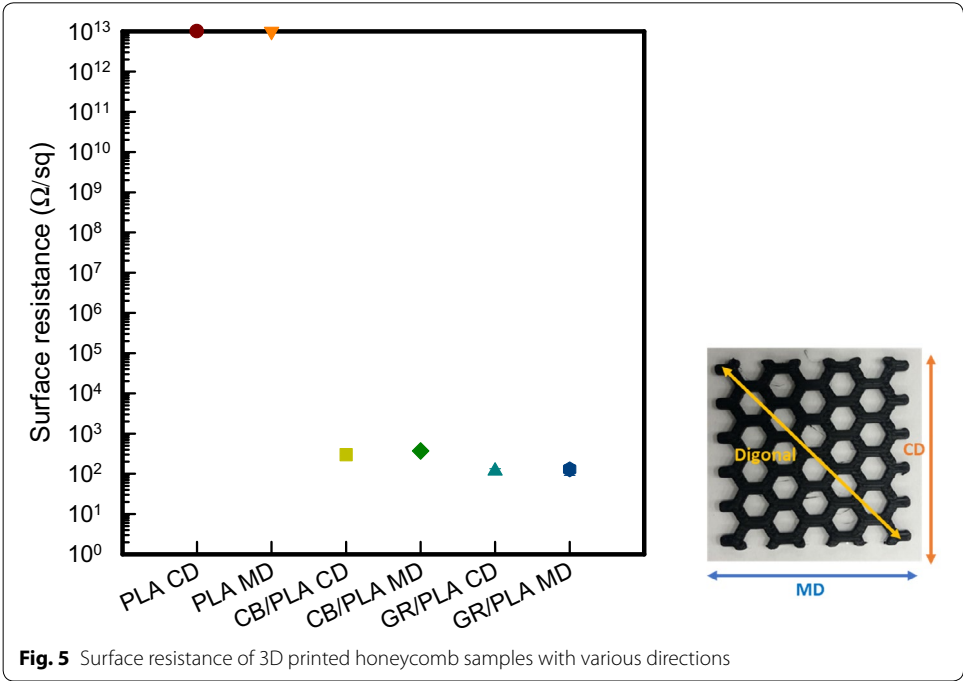
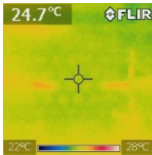
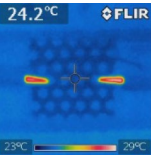
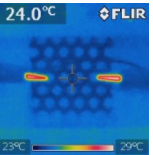
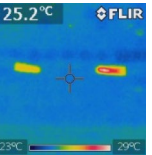
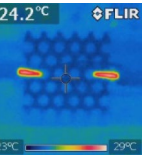
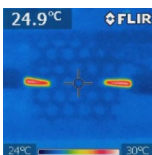
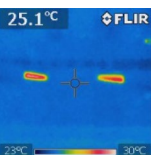
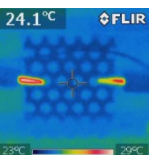
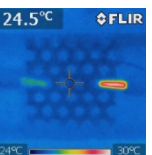
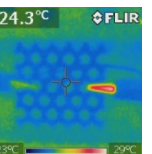


Table 5 Surface resistance of 3D printed honeycomb samples

Direction	Resistance (Ω/sq)		
	PLA	CB/PLA	GR/PLA
CD	> 10 ¹³	299.0 ± 14.6	118.0 ± 15.9
MD	> 10 ¹³	371.7 ± 50.3	129.8 ± 37.8

Table 6 IR images of CD PLA 3D printed honeycomb samples

	Applied voltage (V)				
	5	10	15	20	25
IR image					
Mean Temp. (°C)	26.0 ± 1.9	25.9 ± 1.2	25.9 ± 2.1	26.1 ± 2.0	26.0 ± 2.6
Max Temp. (°C)	31.0 ± 1.4	30.0 ± 0.0	30.0 ± 0.0	30.5 ± 0.7	30.5 ± 0.7
Current (A)	0.00	0.00	0.00	0.00	0.00
	Applied voltage (V)				
	30	35	40	45	50
IR image					
Mean Temp. (°C)	26.0 ± 2.6	26.0 ± 2.3	26.0 ± 2.3	25.7 ± 2.7	26.1 ± 1.8
Max Temp. (°C)	31.0 ± 0.0	30.5 ± 0.7	31.0 ± 0.0	30.5 ± 0.7	30.5 ± 0.7
Current (A)	0.00	0.00	0.00	0.00	0.00

the surface resistance according to the direction. In case of PLA 3D printed honeycomb sample, both directions show over than $10^{13} \Omega/\text{sq}$ by insulation properties of PLA. CB/PLA 3D printed honeycomb sample represents $299.0 \pm 14.6 \Omega/\text{sq}$ and $371.7 \pm 50.3 \Omega/\text{sq}$ in the CD and MD directions, and GR/PLA indicates $118.0 \pm 15.9 \Omega/\text{sq}$ and $129.8 \pm 37.8 \Omega/\text{sq}$, respectively. In this result, it can be observed that the 3D printing process determines the electrical resistivity according to 3D printing direction. Dorigato et al. (2017) reported electrical property under three different direction of 3D printing samples. This study presented that the increase of electrical resistivity is greater for horizontal and vertical printing directions, while is less pronounced for the perpendicular one. It is due to the presence of contact resistances between the deposited filaments by printing direction. In present study, the surface resistivity of CD of both 3D printed honeycomb samples are lower than MD samples. This is probably because more contact resistance occurred when the filaments were deposited into the MD. Thus, it was confirmed that the surface resistance of GR/PLA 3D printed honeycomb sample shows lower value than CB/PLA, the printed CD of 3D printed sample was lower than that of the its MD.

Electrical heating performance of 3D printed honeycomb samples

To analyze the electrical heating performance of 3D printed honeycomb samples using PLA, CB/PLA, and GR/PLA filaments, Tables 5, 6, 7, 8, 9 and 10 indicate IR images of 3D printed honeycomb samples at CD and MD with various applied voltages.

As shown the Tables 6, 8 and 7, PLA 3D printed honeycomb samples at both directions show no electrical heating performance and current with various applied voltages

Table 7 IR images of MD PLA 3D printed honeycomb samples

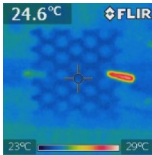
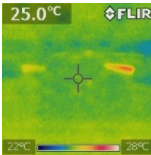
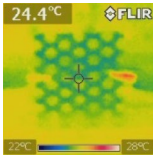
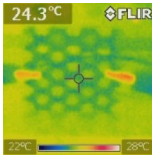
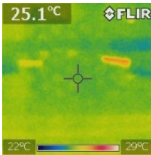
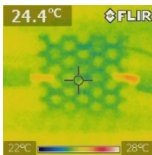
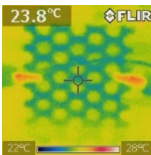
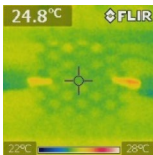
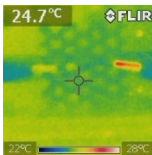
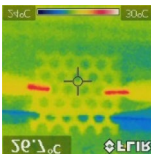
	Applied voltage (V)				
	5	10	15	20	25
IR image					
Mean Temp. (°C)	24.7 ± 0.0	24.2 ± 0.0	24.6 ± 0.8	25.7 ± 0.8	25.2 ± 1.3
Max Temp. (°C)	30.0 ± 1.4	30.0 ± 2.8	29.0 ± 1.4	29.0 ± 1.4	29.5 ± 2.1
Current (A)	0.00	0.00	0.00	0.00	0.00
	Applied voltage (V)				
	30	35	40	45	50
IR image					
Mean Temp. (°C)	25.6 ± 0.9	25.8 ± 1.6	25.3 ± 1.6	25.7 ± 1.7	25.7 ± 1.9
Max Temp. (°C)	29.5 ± 2.1	29.5 ± 2.1	29.5 ± 2.1	29.5 ± 2.1	29.5 ± 2.1
Current (A)	0.00	0.00	0.00	0.00	0.00

Table 8 IR images of CD carbon black/PLA 3D printed honeycomb samples

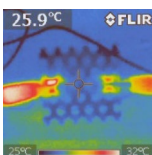
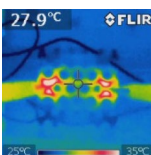
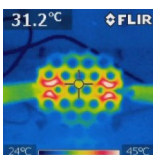
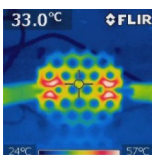
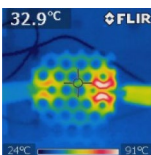
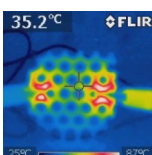
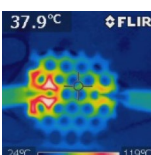
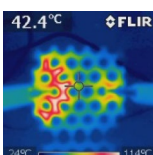
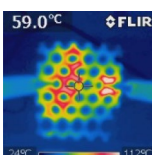
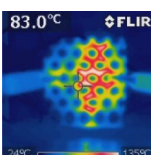
	Applied voltage (V)				
	5	10	15	20	25
IR image					
Mean Temp. (°C)	25.7 ± 0.2	27.4 ± 0.5	30.3 ± 1.1	31.9 ± 1.1	32.6 ± 0.3
Max Temp. (°C)	31.0 ± 1.0	33.7 ± 1.5	43.0 ± 2.6	54.7 ± 6.6	78.7 ± 13.7
Current (A)	0.02 ± 0.01	0.03 ± 0.01	0.05 ± 0.01	0.06 ± 0.01	0.07 ± 0.01
	Applied voltage (V)				
	30	35	40	45	50
IR image					
Mean Temp. (°C)	33.7 ± 1.3	35.8 ± 1.9	38.7 ± 3.2	51.4 ± 8.4	74.2 ± 13.7
Max Temp. (°C)	91.3 ± 4.5	104.0 ± 13.7	117.3 ± 4.2	111.7 ± 4.5	130.7 ± 8.4
Current (A)	0.07 ± 0.01	0.08 ± 0.01	0.09 ± 0.01	0.10 ± 0.01	0.11 ± 0.01

Table 9 IR images of MD carbon black/PLA 3D printed honeycomb samples

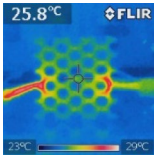
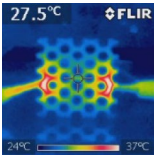
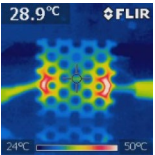
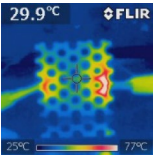
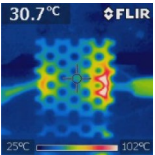
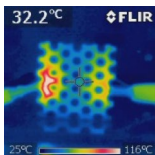
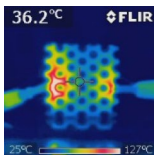
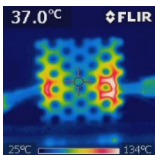
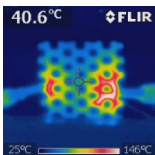
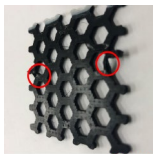
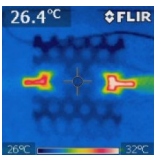
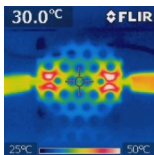
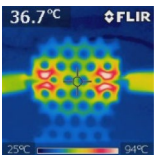
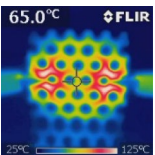
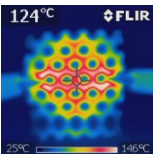
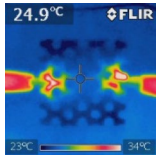
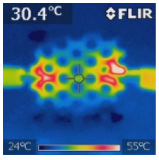
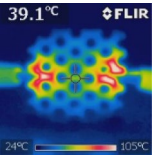
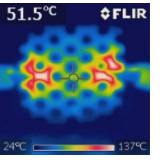
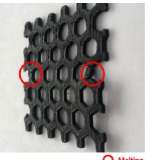
	Applied voltage (V)				
	5	10	15	20	25
IR image					
Mean Temp. (°C)	25.8 ± 0.1	27.3 ± 0.4	29.0 ± 0.1	30.4 ± 0.6	31.6 ± 1.2
Max Temp. (°C)	30.0 ± 1.4	34.5 ± 3.5	45.0 ± 7.1	68.0 ± 12.7	83.0 ± 12.9
Current (A)	0.01 ± 0.0	0.03 ± 0.00	0.05 ± 0.01	0.05 ± 0.01	0.06 ± 0.02
	Applied voltage (V)				
	30	35	40	45	50
IR image					
Mean Temp. (°C)	32.5 ± 0.4	35.8 ± 0.6	37.2 ± 0.2	41.7 ± 4.6	–
Max Temp. (°C)	103.5 ± 6.7	114.0 ± 8.4	120.0 ± 8.5	136.5 ± 7.6	–
Current (A)	0.06 ± 0.01	0.07 ± 0.01	0.08 ± 0.01	0.09 ± 0.01	–

Table 10 IR images of CD graphene/PLA 3D printed honeycomb samples

	Applied voltage (V)				
	5	10	15	20	25
IR image					
Mean Temp. (°C)	25.7 ± 0.9	29.7 ± 1.2	37.7 ± 1.0	61.1 ± 8.2	93.5 ± 21.6
Max Temp. (°C)	32.3 ± 0.5	47.8 ± 2.1	87.3 ± 5.4	128.0 ± 4.2	142.0 ± 4.3
Current (A)	0.06 ± 0.01	0.15 ± 0.01	0.25 ± 0.01	0.39 ± 0.01	0.45 ± 0.03

due to insulation properties of PLA. In case of CB/PLA 3D printed honeycomb samples with both directions, the surface temperature increases with increasing applied voltages. As increasing the applied voltage for each CB/PLA and GR/PLA 3D printed honeycomb sample at cross direction, the distribution of 3D printed honeycomb samples indicates non-uniformly, only both edges represented the electrical heating performance. Also, when applying voltage 50 V for CB/PLA 3D printed honeycomb sample at machine direction, melting was occurred at the point where the power supply was connected. Thus, the mean surface temperature of CD and MD of CB/PLA 3D printed honeycomb sample at 45 V was confirmed as 51.4 ± 8.4 °C and 46.7 ± 4.6 °C, respectively (Tables 8,

Table 11 IR images of MD graphene/PLA 3D printed honeycomb samples

	Applied voltage (V)				
	5	10	15	20	25
IR image					
Mean Temp. (°C)	24.9 ± 0.3	31.5 ± 1.7	41.5 ± 2.0	58.1 ± 8.1	–
Max Temp. (°C)	31.5 ± 0.8	52.5 ± 5.6	96.8 ± 6.2	142.8 ± 5.9	–
Current (A)	0.07 ± 0.01	0.17 ± 0.02	0.27 ± 0.01	0.43 ± 0.03	–

9). Tables 10, 11 shown as IR images of GR/PLA 3D printed honeycomb samples at MD and CD. In case of GR/PLA 3D printed honeycomb samples, the mean surface temperature about 50 °C was occurred below applied voltage at 25 V. GR/PLA 3D printed honeycomb samples also indicated melting at the point where the power supply was connected. When the 20 V was applied to GR/PLA 3D printed honeycomb samples, the mean surface temperatures at CD and MD indicated as 61.1 ± 8.2 °C and 58.1 ± 8.1 °C, respectively. The distribution of GR/PLA 3D honeycomb samples at CD are more uniform than MD 3D honeycomb sample.

In the MD direction, the CB/PLA and GR/PLA 3D printed honeycomb samples showed melting at the edge where they were power supplied, which can be correlated with the melting temperature of the CB/PLA and GR/PLA. As seen above in the DSC curves of the CB/PLA and GR/PLA 3D filaments, the T_m of the two filaments was found to be about 160 °C. In the MD direction of CB/PLA 3D printed honeycomb sample, the maximum surface temperature was 136.5 ± 7.6 °C when the below 45 V was applied, it was confirmed that lower than the T_m . In addition, in the MD direction of the GR/PLA 3D printed honeycomb sample, when 20 V or less was applied, the surface temperature was lower than T_m which was indicated 142.8 ± 5.9 °C. However, at 25 V or higher, the surface temperature was confirmed that higher than T_m . Therefore, the CB/PLA and GR/PLA 3D printed honeycomb samples were found to be maintained without morphological deformation at temperatures below T_m . When comparing CB/PLA and GR/PLA 3D printed honeycomb samples at cross direction, the surface temperature of GR/PLA 3D printed honeycomb samples can be occurred over 50 °C at low voltage than CB/PLA 3D samples (Fig. 6). Also, the distribution of electrical heating zone of GR/PLA 3D printed honeycomb samples is more uniform than CB/PLA 3D printed honeycomb samples. Thus, it shows that the electrical heating performance of GR/PLA 3D printed honeycomb sample is better than CB/PLA 3D printed honeycomb sample.

The current–voltage (I – V) curve of 3D printed honeycomb samples with various directions are shown in Fig. 7. As shown in Fig. 7, PLA 3D printed honeycomb sample indicated no current. The current of CB/PLA 3D printed honeycomb samples at CD and MD represented below 0.11 A as applied from 5 to 50 V. In case of GR/PLA 3D printed honeycomb samples, current of CD and MD samples indicates gradually increase, CD samples were shown as from 0.06 to 0.45 A at from 5 to 25 V and MD samples were

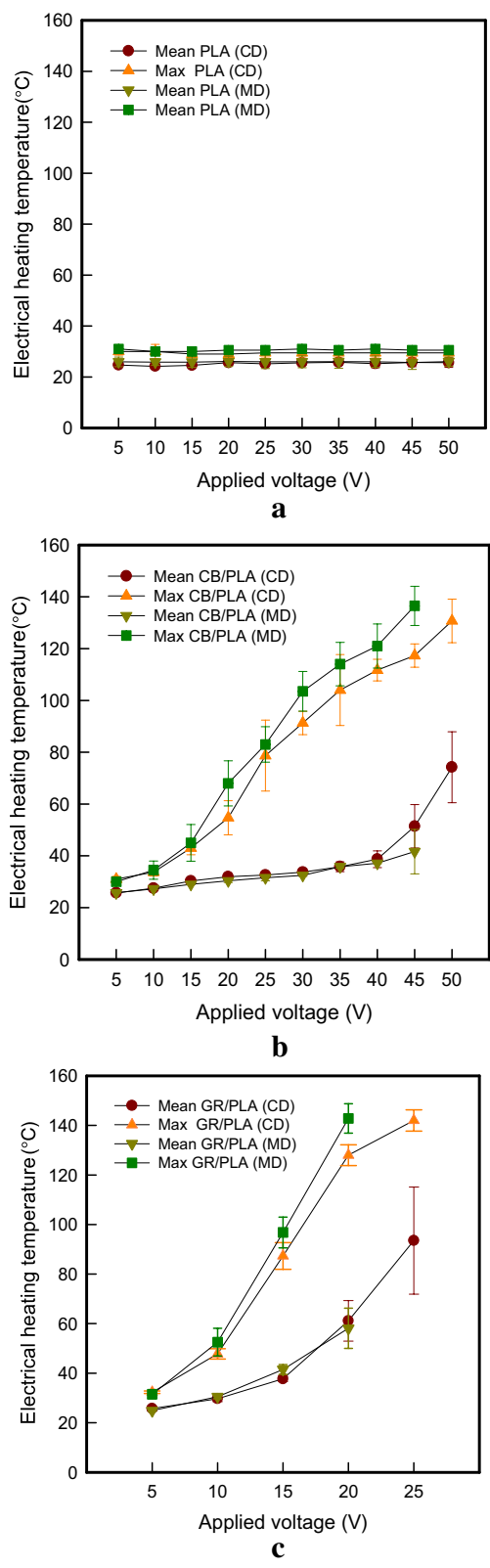


Fig. 6 Surface temperature of 3D printed honeycomb samples of **a** PLA, **b** carbon black/PLA, and **c** graphene/PLA with various directions

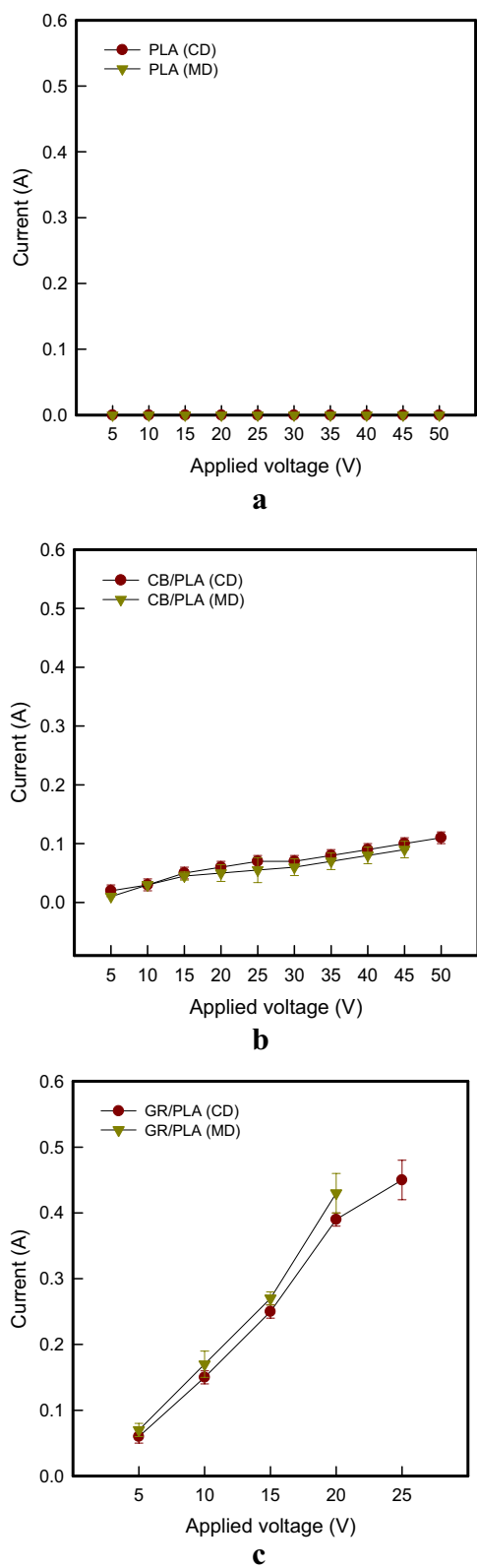


Fig. 7 Current–voltage (I – V) curve of 3D printed honeycomb samples **a** PLA, **b** carbon black/PLA, and **c** graphene/PLA with various directions

represented 0.06 A to 0.43 A at from 5 to 20 V due to melt at 25 V. Thus, in the GR/PLA 3D printed honeycomb samples, it was confirmed that the most current flows.

Generally, electrical heating performance is determined by Joule's law, as shown in Eq. (2),

$$Q = I^2 R t \text{ or } Q = V^2 / R t \quad (2)$$

where Q is the amount of heat, I is the electric current flowing through a conductor, V is the voltage applied across the conductor, R is amount of electric resistance present in the conductor, and t is the amount of time. In each direction, when the same voltage of 45 V was applied to the CB/PLA 3D printed honeycomb sample, the surface resistance of the CD direction was smaller than that of the MD direction, thereby increasing the current. Even when 20 V was applied to the GR/PLA 3D printed honeycomb sample, the same tendency was observed as CB/PLA samples. Surface resistance in the CD direction is smaller than in the MD direction, and thus the current tends to increase. It is confirmed that 3D printed honeycomb samples at CD has better electrical heating performance than the MD. In addition, when applying the same voltage of 20 V at two ends of the CB/PLA or GR/PLA 3D printed honeycomb samples, the surface resistance of GR/PLA 3D printed samples was lower than that of CB/PLA 3D printed samples, and the current was also higher about 7.5 times than CB/PLA 3D printed samples. As a result, the electrical heating performance of GR/PLA 3D printed honeycomb samples was confirmed to be superior to that of CB/PLA 3D printed samples.

Conclusion

This study is a basic research to manufacture a fabric heating element with conveyor fused deposition modeling (CFDM) 3D printed. PLA, CB/PLA, and GR/PLA filaments were collected, and 3D printed honeycomb structure samples were fabricated using those filaments by CFDM 3D printer. The result of thermal properties of PLA, CB/PLA and GR/PLA filament, T_g and T_{cc} of CB/PLA or GR/PLA filament shifted to lower temperature than PLA filament, whereas T_m of CB/PLA or GR/PLA filament shifted to higher temperature compared to the PLA, which is associated with melting of large portion of crystals in composites, which are formed due to the nucleation effect of carbon nanofillers. Based on TGA data, the residue of the CB/PLA and GR/PLA filaments at 230 °C and 220 °C respectively which the temperature during 3D printing processing was higher than around 99%, those are not seriously decomposed and damaged during the 3D printing processing. Raman spectra of CB/PLA filament indicated two broad peaks located at about 1350 cm^{-1} and at 1600 cm^{-1} associated with D band and G band, respectively, and GR/PLA filament shows the three major Raman signals at 1353 cm^{-1} which corresponds D band, at 1587 cm^{-1} which associated G band, and around at 2696 cm^{-1} which corresponds 2D band. The I_D/I_G ratio for GR/PLA revealed lower than CB/PLA indicated, thus, GR/PLA indicated more surface integrity. For the 3D printed honeycomb structure sample using CB/PLA and GR/PLA, the optimum condition was set up 230 °C and 220 °C respectively of the printer temperature, 50 °C of bed temperature, and 30 mm/s of printer speed. Surface resistivity of honeycomb structure sample using CB/PLA and GR/PLA is about

299.0 Ω/sq and 118.0 Ω/sq . The maximum surface temperature of honeycomb structure sample using CB/PLA and GR/PLA is 78.7 °C and 143.0 °C applied to 25 V. As a result, the electrical properties and electrical heating performance of GR/PLA 3D printed honeycomb samples was confirmed to be superior to that of CB/PLA 3D printed samples. In this study, 3D printed honeycomb structure was printed using CB/PLA and GR/PLA filament using CFDM 3D printer, and it was confirmed that it showed electrical and electrical heating characteristics. Therefore, it is expected that the fabric heating element to which the GR/PLA 3D printed honeycomb sample with excellent electric heating performance is applied will be possible.

Acknowledgements

This research was supported by Basic Science Research Program through the National Research Foundation of Korea (NRF) funded by the Ministry of Science, ICT and Future Planning (No. NRF-2016M3A7B4910552).

Authors' contributions

SL conceived the work and SL prepared the samples and HK performed the experiments. HK and SL are participated in the sequence alignment and drafted the manuscript. Both authors read and approved the final manuscript.

Funding

This work was supported by the National Research Foundation of Korea (NRF) Granted funded by the Korea government (MSIP) (No. NRF-2016M3A7B4910552).

Availability of data and materials

The data sets used and analyzed during the current study are available from the corresponding author on reasonable request.

Competing interests

The authors declare that they have no competing interests.

Author details

¹ Graduated Student of the Doctor's Course, Research Institute of Convergence Design, Dong-A University, Busan 49315, South Korea. ² Professor, Department of Fashion Design, Dong-A University, Busan 49315, South Korea.

Received: 23 September 2019 Accepted: 3 January 2020

Published online: 05 March 2020

References

- Azi, P., Soorbaghi, F. P., Azar, A., & Jalali-Arani, A. (2019). Electrical conductivity of graphene filled PLA/PMMA blends: Experimental investigation and modeling. *Polymer Composites*, 40(2), 704–715. <https://doi.org/10.1002/pc.24722>.
- Black belt 3D printer. (2019). Retrieved 29 August 2019 from. <http://blackbelt-3d.com/>
- Bokobza, L., Bruneel, J.-L., & Couzi, M. (2015). Raman spectra of carbon-based materials (from graphite to carbon black) and of some silicone composites. *C*, 1, 77–94. <https://doi.org/10.3390/c1010077>.
- Bokobza, L., Rahmani, M., Belin, C., Bruneel, J.-L., & Bounia, N.-E. E. (2008). Blends of carbon blacks and multiwall carbon nanotubes. *Journal of Polymer Science Part B: Polymer Physics*, 46(18), 1939–1951. <https://doi.org/10.1002/polb.21529>.
- Dorigato, A., Moretti, V., Dul, S., Unterberger, S. H., & Pegoretti, A. (2017). Electrically conductive nanocomposites for fused deposition modelling. *Synthetic Metals*, 226, 7–14. <https://doi.org/10.1016/j.synthmet.2017.01.009>.
- Flowers, P. F., Reyes, C., Ye, S., Kim, H. J., & Wiley, B. J. (2017). 3D printing electronic components and circuits with conductive thermoplastic filament. *Additive Manufacturing*, 18, 156–163. <https://doi.org/10.1016/j.addma.2017.10.002>.
- Foster, C. W., Down, M. P., Zhang, Y., Ji, X., Rowely-Neale, S. J., Smith, G. C., et al. (2017). 3D printed graphene based energy storage devices. *Scientific Reports*, 7(42233), 1–11. <https://doi.org/10.1038/srep42233>.
- Grimmelsmann, N., Kreuziger, M., Korgner, M., Meissner, H., & Ehrmann, A. (2018). Adhesion of 3D printed material on textile substrates. *Rapid Prototyping Journal*, 24(1), 166–179. <https://doi.org/10.1108/RPJ-05-2016-0086>.
- Guo, H., Lv, R., & Bai, S. (2019). Recent advanced on 3D printing graphene-based composites. *Nano Materials Science*, 1, 101–115. <https://doi.org/10.1016/j.nanoms.2019.03.003>.
- Ivanov, E., Kotsilkova, R., Xia, H., Chen, Y., Donato, R. K., Donato, K., et al. (2019). PLA/Graphene/MWCNT composite with improved electrical and thermal properties suitable for FDM 3D printing applications. *Applied Sciences*, 9(1209), 1–14. <https://doi.org/10.3390/app9061209>.
- Kamyshny, A., & Magdassi, S. (2019). Conductive nanomaterials for 2D and 3D printed flexible electronics. *Chemical Society Reviews*, 48, 1712–1740. <https://doi.org/10.1039/c8cs00738a>.
- Kim, S. G., & Kim, H. R. (2018). The recent tendency of fashion textiles by 3D printing. *Fashion & Textile Research Journal*, 20(2), 117–127. <https://doi.org/10.5805/SFTI.2018.20.2.117>.
- Kim, H., & Lee, S. (2018a). Characterization of carbon nanofiber (CNF)/polymer composite coated on cotton fabrics prepared with various circuit patterns. *Fashion and Textiles*, 5(7), 1–13. <https://doi.org/10.1186/s40961-017-0120-2>.
- Kim, H., & Lee, S. (2018b). Characteristics of electrical heating elements coated with graphene nanocomposite on polyester fabric: effect of different graphene contents and annealing temperatures. *Fibers and Polymers*, 9(5), 965–976. <https://doi.org/10.1007/s12221-018-7825-8>.

- Kim, H., & Lee, S. (2019a). Electrical heating properties of various electro-circuit patterns coated on cotton fabric using graphene/polymer composites. *Textile Research Journal*. <https://doi.org/10.1177/0040517519829922>.
- Kim, H., & Lee, S. (2019b). Characterization of electrical heating textile coated by graphene nanoplatelets/PVDF-HFP composite with various high graphene nanoplatelet contents. *Polymers*, 11, 928. <https://doi.org/10.3390/polym11050928>.
- Kim, M. J., Cruz, M. A., Ye, S., Gray, A. L., Smith, G. L., Lazarus, N., et al. (2019a). One-step electrodeposition of copper on conductive 3D printed objects. *Additive Manufacturing*, 27, 318–326. <https://doi.org/10.1016/j.addma.2019.03.016>.
- Kim, H., Lee, S., & Kim, H. (2019b). Electrical heating performance of electro-conductive para-aramid knit manufactured by dip-coating in a graphene/waterborne polyurethane composite. *Scientific Reports*, 9(1511), 1–10. <https://doi.org/10.1038/s41598-37455-0>.
- Kim, S., Seong, H., Her, Y., & Chun, J. (2019c). A study of the development and improvement of fashion products using a FDM type 3D printer. *Fashion and Textiles*, 6(9), 1–24. <https://doi.org/10.1186/s40691-018-0162-0>.
- Kotsilkova, R., Petrova-Doycheva, I., Menseidov, D., Ivanov, E., Paddubskaya, A., & Kuzhir, P. (2019). Exploring thermal annealing and graphene-carbon nanotube additives to enhance crystallinity, thermal, electrical and tensile properties of aged poly(lactic) acid-based filament for 3D printing. *Composites Science and Technology*, 181, 107712.
- Kwok, W., Goh, K. H. H., Tan, Z. D., Tan, S. T. M., Tjiu, W. W., Soh, J. Y., et al. (2015). Electrically conductive filament for 3D-printed circuits and sensors. *Applied Materials Today*, 9, 167–175. <https://doi.org/10.1016/j.apmt.2017.07.001>.
- Ladani, R. B., Wu, S., Kinloch, A. J., Ghorbani, K., Zhang, J., Mouritz, A. P., et al. (2016). Multifunctional properties of epoxy nanocomposites reinforced by aligned nanoscale carbon. *Materials and Design*, 94, 554–564. <https://doi.org/10.1016/j.matdes.2016.01.062>.
- Lee, S. H. (2019). Tensile properties and stiffnesses of 3D-printed lace/voile composite fabrics manufactured by various roller processes. *Textile Science and Engineering*, 56(1), 8–14. <https://doi.org/10.12772/TSE.2019.56.008>.
- Mpofu, N. S., Mwasiagi, J. I., Nkiwane, L. C., & Njuguna, D. (2019). Use of regression to study the effect of fabric parameters on the adhesion of 3D printed PLA polymer onto woven fabrics. *Fashion and Textiles*, 6(24), 1–12. <https://doi.org/10.1186/s40691-019-0180-6>.
- Wei, X., Li, D., Jiang, W., Gu, Z., Wang, X., Zhang, Z., et al. (2015). 3D printable graphene composite. *Scientific Reports*, 5(11181), 1–7. <https://doi.org/10.1038/srep11181>.
- Yu, W. W., Zhang, J., Wu, J. R., Wang, X. Z., & Deng, Y. H. (2017). Incorporation of graphitic nano-filler and poly(lactic acid) in fused deposition modeling. *Journal of Applied Polymer Science*, 47703, 1–11. <https://doi.org/10.1002/APP.44703>.
- Zhang, D., Chi, G., Li, B., Gao, Z., Du, Y., Yao, G., et al. (2016). Fabrication of highly conductive graphene flexible circuits by 3D printing. *Synthetic Metals*, 217, 79–86. <https://doi.org/10.1016/j.synthmet.2016.03.014>.
- Zhuang, Y., Song, W., Ning, G., Sun, X., Sun, Z., Xu, G., et al. (2017). 3D-printing of materials with anisotropic heat distribution using conductive polylactic acid composites. *Materials & Design*, 126, 135–140. <https://doi.org/10.1016/j.matdes.2017.04.047>.

Publisher's Note

Springer Nature remains neutral with regard to jurisdictional claims in published maps and institutional affiliations.

Submit your manuscript to a SpringerOpen[®] journal and benefit from:

- Convenient online submission
- Rigorous peer review
- Open access: articles freely available online
- High visibility within the field
- Retaining the copyright to your article

Submit your next manuscript at ► [springeropen.com](https://www.springeropen.com)
